

This is a repository copy of *Distinct monocyte subset phenotypes in patients with different clinical forms of chronic Chagas disease and seronegative dilated cardiomyopathy*.

White Rose Research Online URL for this paper:

<https://eprints.whiterose.ac.uk/id/eprint/152170/>

Version: Published Version

---

**Article:**

Pérez-Mazliah, Damián E [orcid.org/0000-0002-2156-2585](https://orcid.org/0000-0002-2156-2585), Castro Eiro, Melisa D, Álvarez, María Gabriela et al. (7 more authors) (2018) Distinct monocyte subset phenotypes in patients with different clinical forms of chronic Chagas disease and seronegative dilated cardiomyopathy. PLOS NEGLECTED TROPICAL DISEASES. e0006887. ISSN: 1935-2735

<https://doi.org/10.1371/journal.pntd.0006887>

---

**Reuse**

This article is distributed under the terms of the Creative Commons Attribution (CC BY) licence. This licence allows you to distribute, remix, tweak, and build upon the work, even commercially, as long as you credit the authors for the original work. More information and the full terms of the licence here:

<https://creativecommons.org/licenses/>

**Takedown**

If you consider content in White Rose Research Online to be in breach of UK law, please notify us by emailing [eprints@whiterose.ac.uk](mailto:eprints@whiterose.ac.uk) including the URL of the record and the reason for the withdrawal request.

RESEARCH ARTICLE

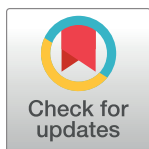
# Distinct monocyte subset phenotypes in patients with different clinical forms of chronic Chagas disease and seronegative dilated cardiomyopathy

Damián E. Pérez-Mazliah<sup>1†</sup>, Melisa D. Castro Eiro<sup>1</sup>, María Gabriela Álvarez<sup>2</sup>, Bruno Lococo<sup>2</sup>, Graciela Bertocchi<sup>2</sup>, Gonzalo César<sup>1</sup>, María A. Natale<sup>1</sup>, María C. Albareda<sup>1</sup>, Rodolfo Viotti<sup>2</sup>, Susana A. Laucella<sup>1\*</sup>

**1** Instituto Nacional de Parasitología Dr. Fátala Chaben, Buenos Aires, Argentina, **2** Hospital Interzonal General de Agudos Eva Perón, Buenos Aires, Argentina

† Current address: The Francis Crick Institute, London, United Kingdom

\* [slaucella@yahoo.com](mailto:slaucella@yahoo.com)



## OPEN ACCESS

**Citation:** Pérez-Mazliah DE, Castro Eiro MD, Álvarez MG, Lococo B, Bertocchi G, César G, et al. (2018) Distinct monocyte subset phenotypes in patients with different clinical forms of chronic Chagas disease and seronegative dilated cardiomyopathy. PLoS Negl Trop Dis 12(10): e0006887. <https://doi.org/10.1371/journal.pntd.0006887>

**Editor:** Carlos A. Buscaglia, Instituto de Investigaciones Biotecnológicas, ARGENTINA

**Received:** February 26, 2018

**Accepted:** October 1, 2018

**Published:** October 22, 2018

**Copyright:** © 2018 Pérez-Mazliah et al. This is an open access article distributed under the terms of the [Creative Commons Attribution License](https://creativecommons.org/licenses/by/4.0/), which permits unrestricted use, distribution, and reproduction in any medium, provided the original author and source are credited.

**Data Availability Statement:** All relevant data are within the paper and its Supporting Information files.

**Funding:** This work was supported by The National Scientific and Technical Research Council, CONICET PIP 2013-037 to SAL and National Fund for Science and Technology Argentina FONCYT, PICT 2005-38188 to SAL. This work was also supported by the National Institute of Health,

## Abstract

### Background

Chronic infection with *Trypanosoma cruzi* leads to a constant stimulation of the host immune system. Monocytes, which are recruited in response to inflammatory signals, are divided into classical CD14<sup>hi</sup>CD16<sup>−</sup>, non-classical CD14<sup>lo</sup>CD16<sup>+</sup> and intermediate CD14<sup>hi</sup>CD16<sup>+</sup> subsets. In this study, we evaluated the frequencies of monocyte subsets in the different clinical stages of chronic Chagas disease in comparison with the monocyte profile of seronegative heart failure subjects and seronegative healthy controls. The effect of the anti-parasite drug therapy benznidazole on monocyte subsets was also explored.

### Methodology/Principal findings

The frequencies of the different monocyte subsets and their phenotypes were measured by flow cytometry. *Trypanosoma cruzi*-specific antibodies were quantified by conventional serological tests. *T. cruzi*-infected subjects with mild or no signs of cardiac disease and patients suffering from dilated cardiomyopathy unrelated to *T. cruzi* infection showed increased levels of non-classical CD14<sup>lo</sup>CD16<sup>+</sup> monocytes compared with healthy controls. In contrast, the monocyte profile in *T. cruzi*-infected subjects with severe cardiomyopathy was skewed towards the classical and intermediate subsets. After benznidazole treatment, non-classical monocytes CD14<sup>lo</sup>CD16<sup>+</sup> decreased while classical monocytes CD14<sup>hi</sup>CD16<sup>−</sup> increased.

### Conclusions/Significance

The different clinical stages of chronic Chagas disease display distinct monocyte profiles that are restored after anti-parasite drug therapy. *T. cruzi*-infected subjects with severe cardiac disease displayed a profile of monocytes subsets suggestive of a more pronounced inflammatory environment compared with subjects suffering from heart failure not related to

Award 110346 to SAL. The funders had no role in study design, data collection and analysis, decision to publish, or preparation of the manuscript.

**Competing interests:** SAL and MCA are members of The National Scientific and Technical Research Council, Argentina. The authors have declared that no competing interests exist.

*T. cruzi* infection, supporting that parasite persistence might also alter cell components of the innate immune system.

## Author summary

Monocytes are key players during infection, and they leave the bloodstream and migrate into tissues in response to inflammatory signals. Although the recruitment of monocytes is essential for the effective control and clearance of microorganisms, they can also be highly damaging to neighboring tissues. Based on the expression of CD14 and CD16, monocytes are classified into classical, non-classical and intermediate subsets, all of which exert different functions. Because chronic *T. cruzi* infection induces a constant activation of the host immune system, inflammatory signals are exacerbated, possibly leading to alterations in the frequencies of monocyte subsets. In this study, we evaluated the monocyte profile in *Trypanosoma cruzi*-infected subjects with different degrees of cardiac dysfunction and explored whether this profile was similar between seropositive and seronegative subjects with heart failure. We found that the different clinical stages of chronic Chagas disease displayed distinct monocyte profiles, which are susceptible to being restored by modulating the parasite load with anti-parasite drug therapy. *T. cruzi*-infected subjects with severe cardiac disease displayed a profile of monocytes subsets suggestive of a more pronounced inflammatory environment compared with subjects suffering from heart failure not related to *T. cruzi* infection, supporting that parasite persistence might be a detrimental factor in the evolution of the cardiac disease induced by *T. cruzi*.

## Introduction

Chagas disease, caused by infection with the intracellular protozoan parasite *Trypanosoma cruzi*, affects 6–7 million people and represents the most frequent cause of infectious cardiomyopathy in the world [1,2]. Three factors are likely associated with the development of the more severe clinical forms of the disease: parasite burden, the capacity of the host immune response to control parasites in specific tissues, and the effectiveness of the host immune response to control tissue damage.

In response to inflammatory signals, circulating monocytes leave the bloodstream and migrate into tissues, where following conditioning by local growth factors, pro-inflammatory cytokines and microbial products, they differentiate into macrophages or dendritic cells. Although the recruitment of monocytes is essential for the effective control and clearance of microorganisms, they can also be highly damaging to neighboring tissues [3]. Human monocytes are divided into subsets on the basis of surface CD14 and CD16 expression [4]. CD14<sup>hi</sup>CD16<sup>−</sup> monocytes “classical Mo”, which are also referred to as classical monocytes, are the most prevalent monocyte subset in human blood, and they show a high expression of the chemokine receptor CCR2. Classical monocytes can migrate to sites of injury and infection, where they differentiate into inflammatory macrophages [5]. The CD16<sup>+</sup> monocyte population comprises two subsets: the non-classical CD14<sup>lo</sup>CD16<sup>+</sup> “non-classical Mo” and the intermediate CD14<sup>hi</sup>CD16<sup>+</sup> monocytes “intermediate Mo” [4,6]. Both subsets exhibit low and mild CCR2 expression [7]. Whereas non-classical monocytes are involved in the process of patrolling with potent anti-inflammatory function and wound healing, intermediate monocytes share some phenotypic and functional features of both classical and non-classical monocytes

and mainly exert a pro-inflammatory role [7]. The two CD16<sup>+</sup> subsets are shown to expand in many inflammatory conditions (e.g., cancer, sepsis and stroke) and infections such as HIV [8–11] and tuberculosis [12].

In the chronic phase of Chagas disease, T cell responses become exhausted over time, presumably due to the constant stimulation of the host immune system in this decades-long infection [13–15]. This constant stimulation of the host immune system is also evident by the expansion of CD14<sup>+</sup>CD16<sup>+</sup>HLA-DR<sup>++</sup> monocytes [16], which shows that adaptive and innate immune responses can be disrupted in the chronic phase of the infection. Chronic Chagas heart disease presents morphological particularities that could account for a worsened clinical course compared with dilated cardiomyopathy not related to *T. cruzi* infection [17].

Herein, we sought to evaluate the frequencies of classical, intermediate and non-classical monocytes in the different clinical stages of chronic Chagas disease compared with the monocyte profile in seronegative dilated cardiomyopathy patients (DCM) and seronegative healthy controls. The effect of the anti-parasite drug therapy benznidazole on monocyte subsets was also explored in chronically infected subjects.

## Materials and methods

### Ethics statement

The protocol was approved by the institutional review boards of Hospital Interzonal General de Agudos Eva Perón, Buenos Aires, Argentina. Signed informed consent was obtained from all individuals before inclusion in the study.

### Study participants

*T. cruzi*-infected adult volunteers were recruited at the Chagas Disease Unit of Hospital Interzonal General de Agudos Eva Perón, Buenos Aires, Argentina. *T. cruzi* infection was determined by indirect immunofluorescence assay, hemagglutination assay, and enzyme-linked immunosorbent assay (ELISA) in compliance with domestic and international criteria [1]. The ELISA was carried out with a 1/200 dilution of the samples incubated in microplates precoated with *T. cruzi* epimastigote antigens. The binding of specific antibodies was detected with a horseradish peroxidase-labeled anti-human IgG antibody (Sigma). After addition of the substrate *o*-phenylenediamine (Sigma), the optical density at 490 nm (OD<sub>490</sub>) was quantified in an ELISA microplate reader (Model 550; Bio-Rad, Tokyo, Japan) [18]. The chronically infected seropositive subjects were clinically evaluated and stratified according to a modified version of the Kuschner grading system [19,20]. The individuals in group 0 had normal electrocardiographic (ECG), normal chest radiographic, and normal echocardiographic findings; the subjects in group 1 had normal chest radiographic and echocardiographic findings but abnormal ECG findings; the subjects in group 2 had ECG abnormalities and heart enlargement; and the subjects in group 3 had ECG abnormalities, heart enlargement, and clinical or radiological evidence of heart failure. A group of seronegative subjects suffering from DCM with systolic heart failure were recruited for comparison of the monocyte subset phenotypes among patients with heart failure due to different disease etiologies. The inclusion criteria for patients with heart failure were class I/II/III (New York Heart Association classification), with an ejection fraction of <40% by echocardiography. The etiology for heart failure was hypertension in three patients, post-chemotherapy with doxorubicin in one patient who had no cancer at the time of study inclusion, alcoholism in one patient, and idiopathic DCM in three patients. Seronegative (uninfected) healthy controls were also included. Subjects with acute coronary syndrome, cancer, HIV, syphilis, diabetes, arthritis, or serious allergies at the time of study inclusion were excluded. At the time of the study, all of the participants were living in Buenos

Table 1. Characteristics of the study population.

| Study group                         | N  | Age range <sup>A</sup><br>(median), years | Years of residence<br>in endemic areas<br>Median (range) | Gender |        |
|-------------------------------------|----|---|--|--------|--------|
|                                     |    |   |  | Male   | Female |
| G0 <sup>B</sup>                     | 23 | 21–60 (43) <sup>C</sup>                   | 18 (1–42)  | 8      | 15     |
| G1 <sup>B</sup>                     | 6  | 24–58 (40)                                | 13 (1–23)  | 5      | 1      |
| G2–G3 <sup>B, D</sup>               | 10 | 46–76 (54) <sup>E</sup>                   | 20 (0–14)  | 8      | 2      |
| Dilated cardiomyopathy <sup>F</sup> | 8  | 34–64 (59)                                | 0  | 7      | 1      |
| Uninfected healthy controls         | 17 | 21–58 (47)                                | 0  | 8      | 9      |

Note.

<sup>A</sup> Age at entry of the study.

<sup>B</sup> Seropositive subjects were grouped according to the modified Kuschner classification [19,20].

<sup>C</sup>  $P < 0.05$  compared with G2–G3 and dilated cardiomyopathy group by ANOVA followed by Bonferroni test.

<sup>D</sup> Three and seven *T. cruzi*-infected subjects were classified as G2 and G3 patients, respectively.

<sup>E</sup>  $P < 0.05$  compared with uninfected healthy controls by ANOVA followed by Bonferroni test.

<sup>F</sup> Seronegative subjects with heart failure and without an epidemiological background for *T. cruzi* infection.

<https://doi.org/10.1371/journal.pntd.0006887.t001>

Aires, where *T. cruzi* infection is not endemic. After inclusion in the study, nine *T. cruzi*-infected subjects in the G0 group and three subjects in the G1 clinical group were treated with 5 mg/kg per day of benznidazole for 30 days [21,22]. Clinical, serological, and immunological analyses were performed prior to and at different time points after the treatment. Data on the number, sex, and age of the enlisted subjects are summarized in Table 1.

### Collection of peripheral blood mononuclear cells (PBMCs) and serum specimens

Whole blood was drawn by venipuncture into heparinized tubes (Vacutainer; BD Biosciences). PBMCs were isolated by density gradient centrifugation on Ficoll-Hypaque (Amersham) and diluted in RPMI media containing 10% newborn bovine serum, 100 units/ml penicillin, 0.1 mg/ml Streptomycin, 2 mM L-glutamine and 10 mM HEPES buffer. The viability of the cells was checked by trypan blue staining with a viability range of 80–90%. A blood aliquot was allowed to coagulate at room temperature and centrifuged at 1000 g for 15 min for serum separation.

### Ex vivo flow cytometry for phenotype analysis

Immediately after collection,  $1 \times 10^6$  PBMCs were stained with different combinations of FITC-labeled anti-CD14, PE-labeled anti-CD16, APC-labeled anti-CD45RA and AF647-labeled anti-CCR2 (all from BD Pharmingen) at 4°C for 30 min. The cells were then fixed with 2% paraformaldehyde and stored at 4°C until acquisition. The cells were acquired with a BD FACS Calibur flow cytometer (BD Biosciences) and analyzed with FlowJo software v9.6 (Tree Star). Monocyte subsets were first selected on the basis of forward-scattered (FSC) vs. side-scattered (SSC) lights, and CD14<sup>+</sup> cells were subsequently gated. From this population, CD14 vs. CD16 dot plots were drawn to establish the different CD14<sup>+</sup> monocyte subsets (S1A, S1B and S1D Fig). For monocyte phenotyping, histograms for the expression of CD45RA and CCR2 were plotted for each monocyte subset (S1E Fig). Unstained and fluorescence minus one (FMO) samples were used as gating controls (S1C and S1E Fig). To demonstrate that the majority of the cells selected by the monocyte gating were truly monocytes, additional analyses were performed as follows. The PerCP-labeled anti-HLA-DR antibody (Biolegend) was added

to the combination of CD14 and CD16 antibodies mentioned above, and CD14 vs. CD16 dot plots were drawn after the selection of HLA-DR<sup>+</sup> cells from the CD14<sup>+</sup>-gated population [23,24] (S1A, S1B, S1E and S1F Fig). Staining with the APC-labeled anti-CD19, APC-Cy7-labeled anti-CD3, PE-labeled anti-CD14, and FITC-labeled anti-CD16 antibodies and with FV510 was performed to ascertain the contribution of any possible contaminating cells, including B, T, to the proportion of the different monocyte subsets. These additional assays were carried out on a FACS Aria II flow cytometer (BD Biosciences; S1 Fig).

## Statistics

The demographic and clinical characteristics of *T. cruzi*-infected subjects included in this study were summarized using the range and median. The normality of data was evaluated by the Shapiro-Wilk test. Differences among groups were evaluated by ANOVA followed by a Bonferroni/Dunn test for multiple comparisons or the Kruskal-Wallis test followed by post-tests, as appropriate. To evaluate the changes in monocyte subsets over time post-treatment compared with the baseline, a linear mixed model with compound symmetry and time as a fixed effect was used to maximize the utilizable data, as some subjects had missing data. The correlation between the frequencies of monocyte subsets and the post-treatment/pre-treatment ratio of *T. cruzi*-specific antibodies measured by ELISA assay was determined by Spearman's test. The networks comprising the different monocyte subsets were created after performing a correlation analysis by Spearman's correlation test. Differences were considered statistically significant at  $P < 0.05$ .

## Results

### Perturbations of monocyte phenotypes in patients with chronic Chagas disease and uninfected subjects with dilated cardiomyopathy

On the basis of the CD14 and CD16 expression levels, CD14<sup>+</sup> monocytes were subdivided into classical (CD14<sup>hi</sup>CD16<sup>-</sup>, "classical Mo"), intermediate (CD14<sup>hi</sup>CD16<sup>+</sup>, "intermediate Mo"), and non-classical (CD14<sup>lo</sup>CD16<sup>+</sup>, "non-classical Mo") subsets (Fig 1A and S1 Fig) and were quantified in untreated *T. cruzi*-infected subjects, seronegative (uninfected) patients with DCM, and in seronegative healthy controls. The frequencies of the different monocyte subsets did not change significantly after preselection of HLA-DR<sup>+</sup> cells from the CD14<sup>+</sup>-gated population (S1A, S1B, S1E and S1F Fig). The preselection of HLA-DR<sup>+</sup> cells allowed for the exclusion of HLA-DR-negative NK cells [23,24]. We confirmed that the contribution of CD3<sup>+</sup> and CD19<sup>+</sup> cells to the frequencies of the different monocyte subsets selected from the total CD14<sup>+</sup>-gated population was very low either in *T. cruzi*-infected or uninfected subjects. As presented in S2 Fig, 1.58% of all CD14<sup>+</sup> monocytes in an uninfected subject showed positive staining for CD19; this figure represents the final frequency of 1.3%, 0.12%, and 0.094% of classical, intermediate, and non-classical monocytes, respectively. Likewise, 2.54% of all CD14<sup>+</sup> monocytes stained for CD3; this percentage represents the final frequency of 1.84%, 0.1%, and 0.072% of classical, intermediate, and non-classical monocytes, respectively.

The frequency of classical monocytes was higher in *T. cruzi*-infected subjects with severe cardiomyopathy (i.e., the G2 and G3 clinical groups) than in patients with no signs of cardiac disease (i.e., the G0 clinical group). Although not statistically significant, patients in groups G2 and G3 had higher frequencies of the CD14<sup>hi</sup>CD16<sup>-</sup> "classical Mo" monocyte subset than those of the uninfected healthy controls and G1 and DCM patients (Fig 1B). In contrast, *T. cruzi*-infected subjects with severe cardiomyopathy had similar frequencies of non-classical CD14<sup>lo</sup>CD16<sup>+</sup> monocytes to the uninfected healthy control levels, whereas *T. cruzi*-infected subjects in the G0 clinical group and patients suffering from DCM unrelated to *T. cruzi*

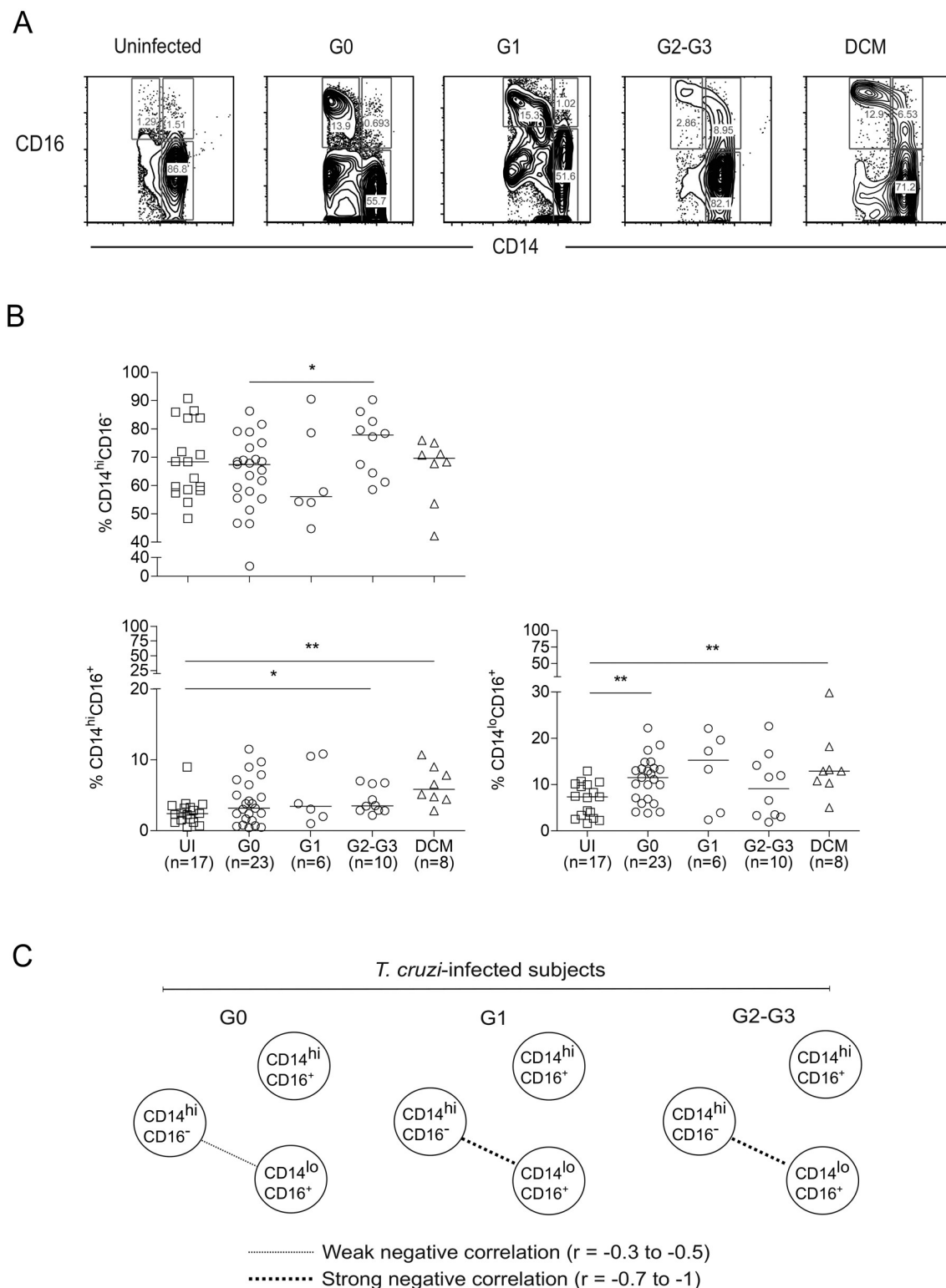


**Fig 1. Measurement of monocyte subsets in chronic Chagas disease patients and seronegative subjects with dilated cardiomyopathy.** (A) Representative plots for single subjects of the different clinical groups (i.e., G0, G1 and G2-G3 patient groups among untreated *T. cruzi*-infected subjects; seronegative subjects with dilated cardiomyopathy (DCM) and uninfected healthy controls) showing CD14 and CD16 expression. Monocytes were selected based on forward (FSC) and side scattering (SSC), and the different CD14<sup>+</sup> monocyte subsets were analyzed by the expression of CD14 and CD16 using flow cytometry. (B) Each point represents the frequency of different monocyte subsets for individual subjects. The median values are indicated by the horizontal lines.

\*  $P < 0.05$ ; \*\*  $P < 0.01$ ; \*\*\*  $P < 0.001$ . Differences among groups were evaluated by ANOVA or the Kruskal-Wallis test followed by post-tests. (C) Classical, intermediate and non-classical monocyte subsets are depicted by the corresponding circles; each connecting line represents a significant interaction ( $P < 0.05$ ) determined by Spearman's correlation test.

<https://doi.org/10.1371/journal.pntd.0006887.g001>

infection (DCM) showed significantly higher levels of non-classical  $CD14^{lo}CD16^{+}$  monocytes than the uninfected healthy controls (Fig 1B). A slight increase in non-classical  $CD14^{lo}CD16^{+}$  monocytes in G1 patients compared with that in the uninfected healthy controls was also observed. Increased frequencies of intermediate  $CD14^{hi}CD16^{+}$  monocytes were found in chronically infected subjects with more severe stages of the disease and DCM compared with the levels in uninfected healthy controls. The  $CD14^{hi}CD16^{+}$  “intermediate Mo” frequencies were also slightly (but not significantly) increased in patients with less severe forms of Chagas disease (Fig 1B). Although patients with chronic Chagas disease with heart failure were older than those in the G0 and the uninfected healthy control groups, we did not find any correlation between the age of the subjects and the frequency of the different monocyte subsets in our study cohort (classical Mo  $r = 0.219$ ,  $P = 0.518$ ; intermediate Mo  $r = -0.002$ ,  $P = 0.996$ ; non-classical Mo  $r = 0.033$ ,  $P = 0.923$ ). A distinct network profile of monocyte subsets was observed in *T. cruzi*-infected subjects that varied according to disease severity. The G0 group, with no signs of cardiac disease, had a moderate inverse correlation between classical  $CD14^{hi}CD16^{-}$  and non-classical  $CD14^{lo}CD16^{+}$  monocyte subsets (Fig 1C). This correlation was not observed in the uninfected healthy controls ( $r = -0.329$ ,  $P = 0.198$ ) or seronegative subjects with DCM ( $r = -0.359$ ,  $P = 0.389$ ). The inverse correlation between classical and non-classical monocyte subsets was increased in the G1 patient group and was sustained in patients with Chagas disease with more severe cardiomyopathy (Fig 1C).

## Phenotyping of the different monocyte subsets

The expression of CD45RA in the different monocyte subsets concurred with the expression data reported in other studies [25–27], and did not vary between patients with chronic Chagas disease regardless the clinical status and uninfected healthy controls (Fig 2A and S1 Fig). In contrast, chronically infected subjects with no signs of cardiac dysfunction had  $CD14^{hi}CD16^{-}$  and  $CD14^{hi}CD16^{+}$  monocyte subsets with higher CCR2 expression than those found in patients with severe cardiac disease and in the uninfected healthy controls, respectively (Fig 2B and S1 Fig).

## Monitoring of monocyte subsets after treatment with benznidazole

To address the relationship between the different monocyte subsets and parasite persistence, classical, non-classical and intermediate monocytes were measured in chronic Chagas disease patients prior to and following treatment with benznidazole. A sharp decrease in non-classical monocytes  $CD14^{lo}CD16^{+}$  along with an increase in classical monocytes  $CD14^{hi}CD16^{-}$  was observed six months after drug therapy (Fig 3A). Of note, the decrease in non-classical monocytes post-treatment was restricted to those patients who had baseline levels above the median values (i.e., non-classical Mo 1 patient group), whereas classical monocytes were increased post-treatment in patients who had baseline  $CD14^{hi}CD16^{-}$  “classical Mo” frequencies under the median values (i.e., classical Mo 2 patient group) (Table 2). Likewise, when patients were classified by those who had baseline frequencies of intermediate  $CD14^{hi}CD16^{+}$  monocytes above (i.e., intermediate Mo 1 patient group) or under (i.e., intermediate Mo 2 patient group) the median values, the frequencies of  $CD14^{hi}CD16^{+}$  “intermediate Mo” decreased in the former group, while the other group presented no changes in this monocyte subset after benznidazole therapy (Table 2). Although the changes were more pronounced at six months post-

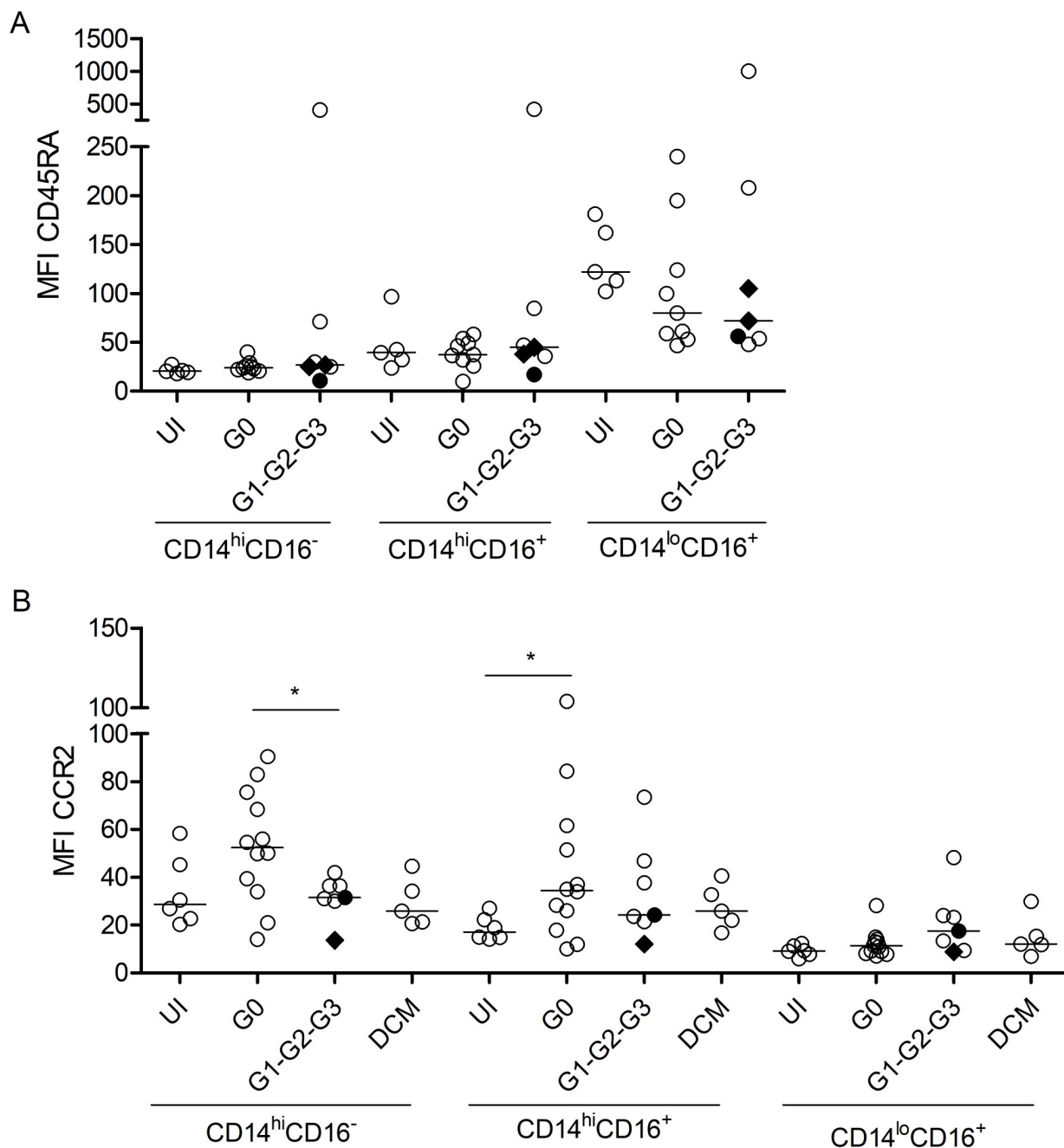


**Fig 2. Phenotyping of the different monocyte subsets.** PBMCs were stained for CD14, CD16, CCR2, HLA-DR and CD45RA and analyzed by flow cytometry. Monocytes were gated by forward and side scattering. Each point represents the MFI for CD45RA (A) and CCR2 (B) in the different monocytes subsets among *T. cruzi*-infected subjects (G0 n = 21; G1-G2-G3 n = 7), seronegative dilated cardiomyopathy patients (DCM) (n = 5) and uninfected healthy controls (n = 6). Black diamonds indicate G1 benznidazole-treated patients; the black circle indicates a G2 benznidazole-treated patient. The median values are indicated by the horizontal lines. \* P < 0.05; Differences among groups were evaluated by ANOVA, the Kruskal-Wallis test followed by post-tests or a t-test.

<https://doi.org/10.1371/journal.pntd.0006887.g002>

treatment, the frequencies of classical and non-classical monocytes were in the range of the uninfected healthy controls (i.e., classical monocytes, range = 48.4%-90.7% and non classical monocytes, range = 1.56%-12.9%) by 12–24 months following drug therapy. Treatment with benznidazole changed the network profile, inducing a positive correlation between classical

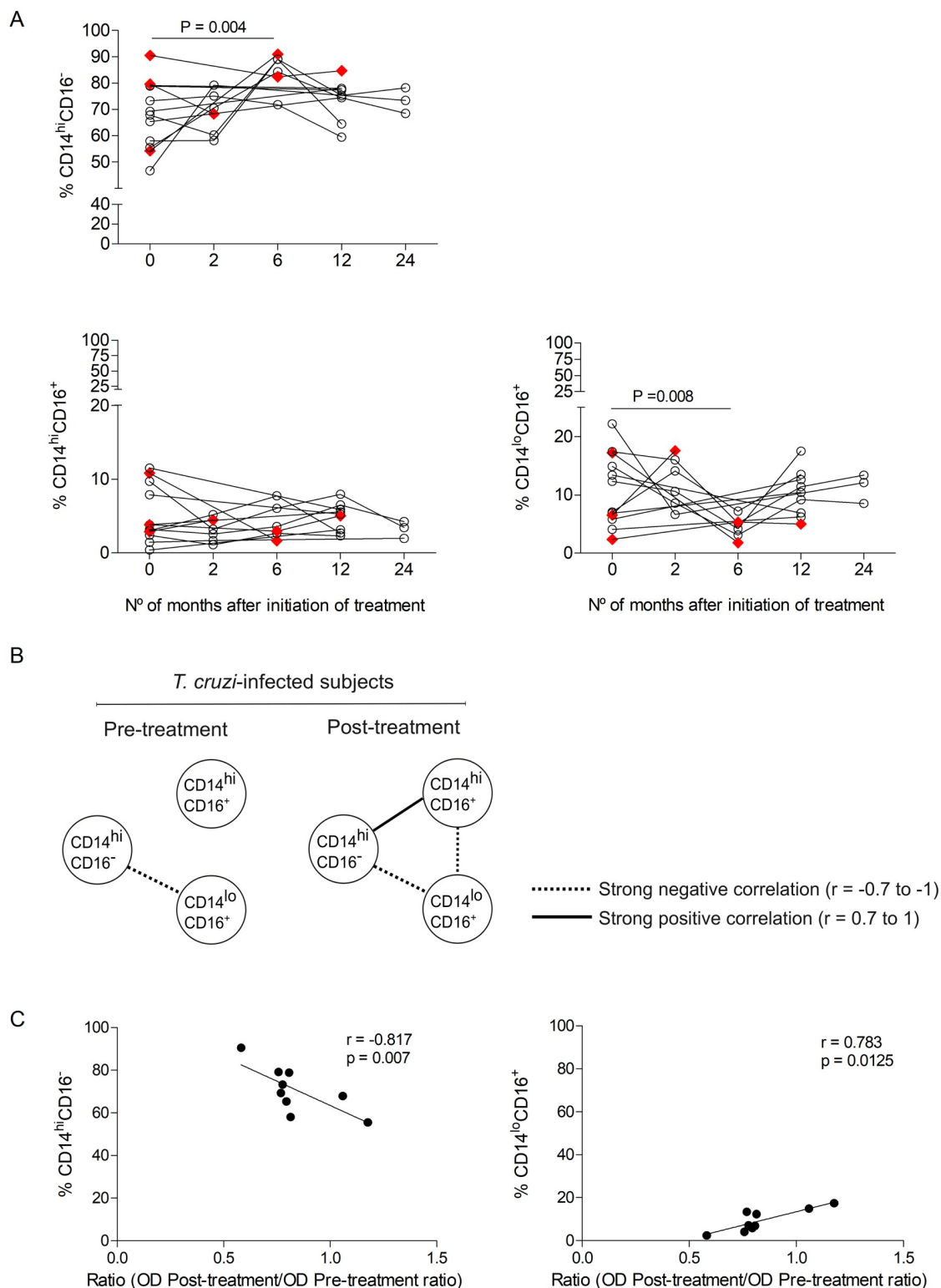


**Fig 3. Monitoring of monocyte subsets after drug therapy in subjects chronically infected with *Trypanosoma cruzi*.** (A) Monocyte subsets were measured prior to and after therapy with benznidazole in 12 *T. cruzi*-infected subjects (G0, black circles; G1, red diamonds). Changes in the monocyte subsets post-treatment relative to baseline were analyzed by a Linear Mixed Model. (B) Classical, intermediate, and non-classical monocyte subsets prior to and after treatment with benznidazole are depicted by the corresponding circles. Each connecting line represents a significant interaction ( $P < 0.05$ ) determined by Spearman's correlation

test. (C) Correlation analysis between the baseline frequencies of classical or non-classical monocyte subsets and the ratio of post-treatment/pre-treatment *T. cruzi*-specific antibodies measured by ELISA at 12–24 months after treatment with benznidazole. Spearman's correlation test between the frequency of CD14<sup>hi</sup>CD16<sup>−</sup> "classical Mo" and CD14<sup>lo</sup>CD16<sup>+</sup> "non-classical Mo" and the post-treatment/pre-treatment ratio of the optical density obtained by the ELISA technique.

<https://doi.org/10.1371/journal.pntd.0006887.g003>

and intermediate monocyte subsets and a strong negative correlation between intermediate and non-classical monocyte subsets within 12–24 months of follow-up post-treatment (Fig 3B). We then evaluated whether the treatment efficacy, determined by the presence of significant decreases in *T. cruzi*-specific antibodies [20], was associated with a particular profile of monocyte subsets prior to drug therapy. An inverse correlation was observed between the

**Table 2. Mixed model analysis of non-classical and intermediate monocyte subsets in chronic Chagas disease patients following therapy with benznidazole according to baseline frequencies.**

| Patient group                 | Dependent variable                                | No. of months Post-treatment | Estimate <sup>A</sup> | 95% CI         | P-value |
|-------------------------------|---|------------------------------|-----------------------|----------------|---------|
| Classical Mo 1<br>(n = 6)     | CD14 <sup>hi</sup> CD16 <sup>−</sup> <sup>B</sup> | Month 2                      | −4.84                 | −18.95, 9.25   | 0.464   |
|                               |   | Month 6                      | −1.14                 | −15.24, 12.96  | 0.861   |
|                               |   | Month 12                     | −3.13                 | −13.65, 7.38   | 0.525   |
| Classical Mo 2<br>(n = 6)     | CD14 <sup>hi</sup> CD16 <sup>−</sup> <sup>C</sup> | Month 2                      | 8.63                  | 0.81, 18.07    | 0.071   |
|                               |   | Month 6                      | 29.24                 | 19.81, 38.68   | < 0.001 |
|                               |   | Month 12                     | 13.05                 | 3.61, 22.48    | 0.010   |
|                               |   | Month 24                     | 16.96                 | 6.59, 27.34    | 0.004   |
| Intermediate Mo 1<br>(n = 6)  | CD14 <sup>hi</sup> CD16 <sup>+</sup> <sup>B</sup> | Month 2                      | −10.36                | −15.81, −4.93  | 0.001   |
|                               |   | Month 6                      | −15.57                | −20.99, −10.14 | < 0.001 |
|                               |   | Month 12                     | −6.04                 | −11.33, −0.76  | 0.028   |
|                               |   | Month 24                     | −8.43                 | −14.08, −2.77  | 0.006   |
| Intermediate Mo 2<br>(n = 6)  | CD14 <sup>hi</sup> CD16 <sup>+</sup> <sup>C</sup> | Month 2                      | 0.38                  | −1.60, 2.36    | 0.69    |
|                               |   | Month 6                      | 1.61                  | −0.52, 3.73    | 0.13    |
|                               |   | Month 12                     | 1.56                  | −0.32, 3.44    | 0.098   |
|                               |   | Month 24                     | 0.53                  | −2.20, 3.26    | 0.69    |
| Non-classical Mo 1<br>(n = 6) | CD14 <sup>lo</sup> CD16 <sup>+</sup> <sup>B</sup> | Month 2                      | −6.22                 | −10.94, −1.52  | 0.013   |
|                               |   | Month 6                      | −13.18                | −17.87, −8.48  | < 0.001 |
|                               |   | Month 12                     | −5.26                 | −9.95, −0.56   | 0.031   |
|                               |   | Month 24                     | −4.94                 | −10.01, 0.14   | 0.050   |
| Non-classical Mo 2<br>(n = 6) | CD14 <sup>lo</sup> CD16 <sup>+</sup> <sup>C</sup> | Month 2                      | 10.46                 | 5.52, −15.40   | 0.001   |
|                               |   | Month 6                      | 0.77                  | −4.16, 5.71    | 0.737   |
|                               |   | Month 12                     | 4.07                  | 0.41, 7.74     | 0.032   |

Note.

<sup>A</sup> The estimate value for each time point post-treatment obtained by linear mixed model analysis indicates an approximation of the fold-change compared with the baseline. Negative values denote a decrease in the frequency of the indicated monocyte subset while positive values denote an increase in the frequency of the indicated monocyte subset compared with baseline;

<sup>B</sup> Subjects with frequencies of the indicated monocyte subset above median values (i.e., patient group 1);

<sup>C</sup> Subjects with frequencies of the indicated monocyte subset under median values (i.e., patient group 2).

<https://doi.org/10.1371/journal.pntd.0006887.t002>

frequencies of classical monocytes prior to treatment and the rate of decreases in *T. cruzi*-specific antibodies post-treatment (i.e., a lower ratio post-treatment vs. pre-treatment in subjects with high baseline frequencies of classical monocytes) (Fig 3C, S3 Fig). In contrast, the frequencies of non-classical monocytes prior to treatment were positively correlated with the decrease in parasite-specific antibodies post-treatment (Fig 3C) (i.e., a lower ratio post-treatment vs. pre-treatment in subjects with low baseline frequencies of non-classical monocytes).

## Discussion

Although the cause of morbidity in chronic *T. cruzi* infection has been the source of much debate and controversy, most of the available data support the conclusion that Chagas disease is the result of the failure of the immune system to completely clear this persistent infection and the resulting effects of decades of immune assault [28,29].

In the present study, we found that the monocyte profile in chronically *T. cruzi*-infected subjects varies according to disease severity and changes after anti-*T. cruzi* treatment with benznidazole. The monocyte profile in less severe forms of cardiac disease is enriched in non-classical monocytes (CD14<sup>lo</sup>CD16<sup>+</sup>), whereas the monocyte profile in Chagas disease patients with severe cardiomyopathy is skewed toward classical and intermediate monocytes. These findings suggest that patients without signs of cardiac dysfunction or mild cardiac disease have a more balanced monocyte profile with both proinflammatory and anti-inflammatory tissue repair capacity [5]. Recent studies revealed that classical monocytes exit from bone marrow into the blood stream, where they give rise to intermediate monocytes, which subsequently differentiate into non-classical monocytes [11,30]. Other authors have reported that non-classical monocytes may also arise independently from myeloid progenitors in the bone marrow [31]. The inverse correlation between classical and non-classical monocytes in chronically *T. cruzi*-infected subjects suggests that non-classical monocytes may derive from classical monocytes. Nonetheless, this inverse association may also be due to more active recruitment of classical than non-classical monocytes in *T. cruzi*-infected tissues in the G0 and G1 groups. In line with these findings, the enhanced expression of CCR2 in classical and intermediate monocytes of *T. cruzi*-infected patients without signs of cardiac disease may support more active recruitment of these monocyte subsets.

Upon activation, classical monocytes produce inflammatory cytokines, may exert phagocytic and myeloperoxidase activities, and release heightened levels of superoxide [32]; these actions altogether can help to keep the parasite under control. Although these responses maintained over time may also result in tissue damage, the recruitment of non-classical monocytes may counteract these harmful effects. In contrast, a more inflammatory environment and tissue damage observed in patients with severe stages of chronic Chagas disease may be responsible for more active chemoattraction and recruitment of non-classical monocytes to sites of inflammation to perform their anti-inflammatory and tissue repair functions [5], accounting for the stronger inverse correlation between classical and non-classical monocytes in these patients. The extensive fibrosis observed in Chagas disease patients with heart failure might be a consequence of exacerbated remodeling [33] mediated by the tissue repair function of non-classical monocytes. Of note, no correlation between classical and non-classical monocytes was observed in DCM, in agreement with the low-grade inflammation associated with heart failure of non-infectious origin [34]. Several studies suggest that *T. cruzi*-infected subjects with an indeterminate form of the chronic disease have an overall modulatory cytokine profile of monocytes, with the production of IL-10 as a counterbalance cytokine [16,35–40]. In line with our findings, a recent study revealed that chronically *T. cruzi*-infected subjects with cardiac dysfunction have an increased frequency of intermediate monocytes [41]. Nevertheless, the

increased counts of both non-classical monocytes at less severe clinical stages in our study are at odds with the results reported by other authors [40,41].

Treatment with benznidazole induced reductions in both non-classical and intermediate monocyte subsets along with an increase in classical-monocyte numbers. This finding is probably due to a reduction in parasite load and the subsequent decrease in inflammation and recruitment of non-classical and intermediate monocytes, thus enabling replenishment of classical monocyte subsets in the circulation. The inverse correlation between non-classical and intermediate monocytes after benznidazole therapy suggests that the signals that induce the rise in the number of non-classical monocytes in the G0 and G1 clinical groups, which are the target populations for trypanocidal treatment, may disappear after this therapy. It has been shown that monocytes can be reprogrammed and switch from a wound-healing to a pro-inflammatory state in response to changes in inflammatory stimuli [42,43]. Accordingly, we recently observed that the levels of MCP-1, one of the main chemokines that regulate migration and infiltration of monocytes and/or macrophages, and of IP-10, which acts as a modulator of angiogenesis and wound healing, decrease in *T. cruzi*-infected children after treatment with benznidazole (Albareda MC, personal communication). In contrast to our findings, Sathler-Avelar et al. demonstrated that a pediatric population of *T. cruzi*-infected subjects treated with benznidazole has higher percentages of non-classical CD14<sup>+</sup>CD16<sup>+</sup> cells as compared with an untreated group [44]. These two studies have several distinct features that might explain these apparent discrepancies, including the difference in the classification of monocytes and in the length of infection. Benznidazole treatment in the indeterminate phase of *T. cruzi* infection has been reported to downregulate monocyte phagocytic capacity [45], further supporting the overall low immune activation after benznidazole therapy. An important observation of our work is that the decline in *T. cruzi*-specific antibody levels after benznidazole therapy, suggestive of successful treatment, was associated with lower baseline levels of non-classical monocytes and higher baseline levels of classical monocytes. A proper balance among the different monocyte subsets may be critical for preventing persistent inflammation and for achieving controlled repair, which might also be an important factor for treatment efficacy.

One limitation of this study is that the functional status of the different monocyte subsets was not assessed prior to and after therapy. Additionally, the gating strategy employed did not allow us to exclude the low frequencies of contaminating B and T cells in the different CD14<sup>+</sup> monocyte subsets.

In summary, *T. cruzi*-infected subjects with severe cardiac disease have a profile of monocyte subpopulations that is suggestive of a more pronounced inflammatory environment as compared with the subjects without signs of cardiac dysfunction and those with heart failure not related to *T. cruzi* infection. These findings further indicate that parasite persistence may also alter cell components of the innate immune system.

## Supporting information

**S1 Fig. Gating strategy.** Monocytes were selected on the basis of forward (FSC) and side (SSC) scatter of light. CD14<sup>+</sup> cells were subsequently selected and analyzed for the different monocyte subsets according to the expression of CD14 and CD16 (A-C). Alternatively, a gate on HLA-DR<sup>+</sup> cells was drawn and the different monocyte subsets were analyzed (A, B, E and F). Classical, intermediate, and non-classical monocytes are gated in green, blue, and red, respectively. For each subset, the expression of CCR2, and CD45RA was analyzed with histogram plots (D). Unstained and fluorescence minus one (FMO) controls were used to determine the nonspecific antibody binding (D, E). (TIF)

### S2 Fig. Multiparametric flow cytometry analysis for identification of truly monocytes.

Monocytes were selected on the basis of forward (FSC) and side (SSC) scattering (A). Viable cells were gated by their negative staining for the viability marker FV510 (B) and single cells were gated based on FSC-W and FSC-A parameters (C). CD14<sup>+</sup> cells were subsequently selected (D) and the different monocyte subsets were drawn according to the expression of CD14 and CD16 (E). Alternatively CD19<sup>+</sup> (F-G) or CD3<sup>+</sup> (H-I) cells were selected from the CD14<sup>+</sup> gate and the different monocyte subsets were drawn as shown in E. The percentages indicate the frequencies of each monocyte subset out of total CD14<sup>+</sup> (E), CD14<sup>+</sup>CD19<sup>+</sup> (G) and CD14<sup>+</sup>CD3<sup>+</sup> (I) cells in an uninfected subject.

(TIF)

### S3 Fig. Monitoring of *Trypanosoma cruzi*-specific antibodies by conventional serological tests following treatment with benznidazole.

*T. cruzi*-specific antibodies, as determined by ELISA (A), hemagglutination assay (B), and immunofluorescence assays (C), were measured prior to and at different time points after the treatment with benznidazole. Each open circle represents the data for single subjects. Broken horizontal lines show the threshold of reactivity for each serological test. \*  $P < 0.05$  versus OD values prior to the treatment, by paired Student's *t*-test.

## Author Contributions

**Conceptualization:** Damián E. Pérez-Mazliah, Susana A. Laucella.

**Data curation:** Damián E. Pérez-Mazliah, María Gabriela Álvarez, Bruno Lococo, Graciela Bertocchi, Rodolfo Viotti, Susana A. Laucella.

**Formal analysis:** Damián E. Pérez-Mazliah, Melisa D. Castro Eiro, Gonzalo César, Susana A. Laucella.

**Funding acquisition:** Susana A. Laucella.

**Investigation:** Damián E. Pérez-Mazliah, Melisa D. Castro Eiro, Bruno Lococo, Graciela Bertocchi, Gonzalo César, María A. Natale, María C. Albareda, Rodolfo Viotti, Susana A. Laucella.

**Methodology:** Damián E. Pérez-Mazliah, María Gabriela Álvarez, Susana A. Laucella.

**Project administration:** Susana A. Laucella.

**Resources:** Susana A. Laucella.

**Supervision:** Susana A. Laucella.

**Writing – original draft:** Melisa D. Castro Eiro, María A. Natale, María C. Albareda, Susana A. Laucella.

**Writing – review & editing:** Damián E. Pérez-Mazliah, Melisa D. Castro Eiro, María Gabriela Álvarez, Bruno Lococo, Graciela Bertocchi, Gonzalo César, María A. Natale, María C. Albareda, Rodolfo Viotti, Susana A. Laucella.

## References

1. TDR/WHO. Research Priorities for Chagas Disease, Human African Trypanosomiasis and Leishmaniasis. WHO Tech Rep Ser. 2012;
2. Feldman AM, McNamara D. Myocarditis. N Engl J Med. Massachusetts Medical Society; 2000; 343: 1388–98. <https://doi.org/10.1056/NEJM200011093431908> PMID: 11070105

3. Auffray C, Sieweke MH, Geissmann F. Blood monocytes: development, heterogeneity, and relationship with dendritic cells. *Annu Rev Immunol*. Annual Reviews; 2009; 27: 669–92. <https://doi.org/10.1146/annurev.immunol.021908.132557> PMID: 19132917
4. Ziegler-Heitbrock L. Blood Monocytes and Their Subsets: Established Features and Open Questions. *Front Immunol*. 2015; 6: 423. <https://doi.org/10.3389/fimmu.2015.00423> PMID: 26347746
5. Thomas G, Tacke R, Hedrick CC, Hanna RN. Nonclassical patrolling monocyte function in the vasculature. *Arterioscler Thromb Vasc Biol*. 2015; 35: 1306–16. <https://doi.org/10.1161/ATVBAHA.114.304650> PMID: 25838429
6. Ziegler-Heitbrock L, Ancuta P, Crowe S, Dalod M, Grau V, Hart DN, et al. Nomenclature of monocytes and dendritic cells in blood. *Blood*. 2010; 116: e74–80. <https://doi.org/10.1182/blood-2010-02-258558> PMID: 20628149
7. Cros J, Cagnard N, Woollard K, Patey N, Zhang S-Y, Senechal B, et al. Human CD14dim monocytes patrol and sense nucleic acids and viruses via TLR7 and TLR8 receptors. *Immunity*. 2010; 33: 375–86. <https://doi.org/10.1016/j.immuni.2010.08.012> PMID: 20832340
8. Chen P, Su B, Zhang T, Zhu X, Xia W, Fu Y, et al. Perturbations of Monocyte Subsets and Their Association with T Helper Cell Differentiation in Acute and Chronic HIV-1-Infected Patients. *Front Immunol*. 2017; 8: 272. <https://doi.org/10.3389/fimmu.2017.00272> PMID: 28348563
9. Funderburg NT, Zidar DA, Shive C, Lioi A, Mudd J, Musselwhite LW, et al. Shared monocyte subset phenotypes in HIV-1 infection and in uninfected subjects with acute coronary syndrome. *Blood*. 2012; 120: 4599–608. <https://doi.org/10.1182/blood-2012-05-433946> PMID: 23065151
10. Hanna RN, Cekic C, Sag D, Tacke R, Thomas GD, Nowyhed H, et al. Patrolling monocytes control tumor metastasis to the lung. *Science*. 2015; 350: 985–90. <https://doi.org/10.1126/science.aac9407> PMID: 26494174
11. Yang J, Zhang L, Yu C, Yang X-F, Wang H. Monocyte and macrophage differentiation: circulation inflammatory monocyte as biomarker for inflammatory diseases. *Biomark Res*. 2014; 2: 1. <https://doi.org/10.1186/2050-7771-2-1> PMID: 24398220
12. Castaño D, García LF, Rojas M. Increased frequency and cell death of CD16+ monocytes with *Mycobacterium tuberculosis* infection. *Tuberculosis (Edinb)*. Elsevier; 2011; 91: 348–60. <https://doi.org/10.1016/j.tube.2011.04.002> PMID: 21621464
13. Laucella SA, Postan M, Martin D, Hubby Fralish B, Albareda MC, Alvarez MG, et al. Frequency of interferon- gamma -producing T cells specific for *Trypanosoma cruzi* inversely correlates with disease severity in chronic human Chagas disease. *J Infect Dis*. 2004; 189: 909–18. <https://doi.org/10.1086/381682> PMID: 14976609
14. Albareda MC, Laucella SA, Alvarez MG, Armenti AH, Bertochi G, Tarleton RL, et al. *Trypanosoma cruzi* modulates the profile of memory CD8+ T cells in chronic Chagas' disease patients. *Int Immunol*. 2006; 18: 465–71. <https://doi.org/10.1093/intimm/dxh387> PMID: 16431876
15. Argüello RJ, Balbaryski J, Barboni G, Candi M, Gaddi E, Laucella S. Altered frequency and phenotype of CD4+ forkhead box protein 3+ T cells and its association with autoantibody production in human immunodeficiency virus-infected paediatric patients. *Clin Exp Immunol*. 2012; 168: 224–33. <https://doi.org/10.1111/j.1365-2249.2012.04569.x> PMID: 22471284
16. Vitelli-Avelar DM, Sathler-Avelar R, Massara RL, Borges JD, Lage PS, Lana M, et al. Are increased frequency of macrophage-like and natural killer (NK) cells, together with high levels of NKT and CD4+ CD25high T cells balancing activated CD8+ T cells, the key to control Chagas' disease morbidity? *Clin Exp Immunol*. 2006; 145: 81–92. <https://doi.org/10.1111/j.1365-2249.2006.03123.x> PMID: 16792677
17. Bestetti RB, Muccillo G. Clinical course of Chagas' heart disease: a comparison with dilated cardiomyopathy. *Int J Cardiol*. 1997; 60: 187–93. Available: <http://www.ncbi.nlm.nih.gov/pubmed/9226290> PMID: 9226290
18. García MM, De Rissio AM, Villalonga X, Mengoni E, Cardoni RL. Soluble tumor necrosis factor (TNF) receptors (sTNF-R1 and -R2) in pregnant women chronically infected with *Trypanosoma cruzi* and their children. *Am J Trop Med Hyg*. 2008; 78: 499–503. Available: <http://www.ncbi.nlm.nih.gov/pubmed/18337349> PMID: 18337349
19. Kuschner E, Sgammini H, Castro R, Evequoz C, Ledesma R, Brunetto J. [Evaluation of cardiac function by radioisotopic angiography, in patients with chronic Chagas cardiopathy]. *Arq Bras Cardiol*. 1985; 45: 249–56. Available: <http://www.ncbi.nlm.nih.gov/pubmed/3835868> PMID: 3835868
20. Viotti R, Vigliano C, Alvarez MG, Lococo B, Petti M, Bertocchi G, et al. Impact of aetiological treatment on conventional and multiplex serology in chronic Chagas disease. *PLoS Negl Trop Dis*. 2011; 5: e1314. <https://doi.org/10.1371/journal.pntd.0001314> PMID: 21909451
21. Viotti R, Vigliano C, Armenti H, Segura E. Treatment of chronic Chagas' disease with benznidazole: clinical and serologic evolution of patients with long-term follow-up. *Am Heart J*. Elsevier; 1994; 127: 151–62. [https://doi.org/10.1016/0002-8703\(94\)90521-5](https://doi.org/10.1016/0002-8703(94)90521-5)

22. Viotti R, Vigliano C, Lococo B, Petti M, Bertocchi G, De Cecco F, et al. Exercise stress testing as a predictor of progression of early chronic Chagas heart disease. *Heart*. 2006; 92: 403–4. <https://doi.org/10.1136/hrt.2005.064444> PMID: 16501205
23. Abeles RD, McPhail MJ, Sowter D, Antoniadis CG, Vergis N, Vijay GKM, et al. CD14, CD16 and HLA-DR reliably identifies human monocytes and their subsets in the context of pathologically reduced HLA-DR expression by CD14(hi)/CD16(neg) monocytes: Expansion of CD14(hi)/CD16(pos) and contraction of CD14(lo)/CD16(pos) monocytes in a. *Cytometry A*. 2012; 81: 823–34. <https://doi.org/10.1002/cyto.a.22104> PMID: 22837127
24. Leers MPG, Stockem C, Ackermans D, Loeffen R, Ten Cate H, Kragten JA, et al. Intermediate and non-classical monocytes show heterogeneity in patients with different types of acute coronary syndrome. *Cytometry A*. 2017; 91: 1059–1067. <https://doi.org/10.1002/cyto.a.23263> PMID: 29024334
25. Rothe G, Gabriel H, Kovacs E, Klucken J, Stöhr J, Kindermann W, et al. Peripheral blood mononuclear phagocyte subpopulations as cellular markers in hypercholesterolemia. *Arterioscler Thromb Vasc Biol*. 1996; 16: 1437–47. Available: <http://www.ncbi.nlm.nih.gov/pubmed/8977447> PMID: 8977447
26. Allan DS, Colonna M, Lanier LL, Churakova TD, Abrams JS, Ellis SA, et al. Tetrameric complexes of human histocompatibility leukocyte antigen (HLA)-G bind to peripheral blood myelomonocytic cells. *J Exp Med*. 1999; 189: 1149–56. Available: <http://www.ncbi.nlm.nih.gov/pubmed/10190906> PMID: 10190906
27. Brohée D, Higuier N. In vitro stimulation of peripheral blood mononuclear cells by phytohaemagglutinin A induces CD45RA expression on monocytes. *Cytobios*. 1992; 71: 105–11. Available: <http://www.ncbi.nlm.nih.gov/pubmed/1473353> PMID: 1473353
28. Tarleton RL. Chagas disease: a role for autoimmunity? *Trends Parasitol*. Elsevier; 2003; 19: 447–51. <https://doi.org/10.1016/j.pt.2003.08.008>
29. Albareda MC, Laucella SA. Modulation of *Trypanosoma cruzi*-specific T-cell responses after chemotherapy for chronic Chagas disease. *Mem Inst Oswaldo Cruz*. Instituto Oswaldo Cruz, Ministério da Saúde; 2015; 110: 414–21. <https://doi.org/10.1590/0074-02760140386> PMID: 25993507
30. Patel AA, Zhang Y, Fullerton JN, Boelen L, Rongvaux A, Maini AA, et al. The fate and lifespan of human monocyte subsets in steady state and systemic inflammation. *J Exp Med*. 2017; 214: 1913–1923. <https://doi.org/10.1084/jem.20170355> PMID: 28606987
31. Geissmann F, Auffray C, Palframan R, Wirth C, Ciocca A, Campisi L, et al. Blood monocytes: distinct subsets, how they relate to dendritic cells, and their possible roles in the regulation of T-cell responses. *Immunol Cell Biol*. Australasian Society for Immunology Inc.; 2008; 86: 398–408. <https://doi.org/10.1038/icb.2008.19> PMID: 18392044
32. Qu C, Brinck-Jensen N-S, Zang M, Chen K. Monocyte-derived dendritic cells: targets as potent antigen-presenting cells for the design of vaccines against infectious diseases. *Int J Infect Dis*. 2014; 19: 1–5. <https://doi.org/10.1016/j.ijid.2013.09.023> PMID: 24216295
33. Barretto AC, Higuchi ML, da Luz PL, Lopes EA, Bellotti G, Mady C, et al. [Comparison of histologic changes in Chagas' cardiomyopathy and dilated cardiomyopathy]. *Arq Bras Cardiol*. 1989; 52: 79–83. Available: <http://www.ncbi.nlm.nih.gov/pubmed/2596992> PMID: 2596992
34. Anker SD, Egerer KR, Volk HD, Kox WJ, Poole-Wilson PA, Coats AJ. Elevated soluble CD14 receptors and altered cytokines in chronic heart failure. *Am J Cardiol*. Elsevier; 1997; 79: 1426–30. [https://doi.org/10.1016/S0002-9149\(97\)00159-8](https://doi.org/10.1016/S0002-9149(97)00159-8)
35. Medeiros NI, Fares RCG, Franco EP, Sousa GR, Mattos RT, Chaves AT, et al. Differential Expression of Matrix Metalloproteinases 2, 9 and Cytokines by Neutrophils and Monocytes in the Clinical Forms of Chagas Disease. *PLoS Negl Trop Dis*. 2017; 11: e0005284. <https://doi.org/10.1371/journal.pntd.0005284> PMID: 28118356
36. Souza PEA, Rocha MOC, Menezes CAS, Coelho JS, Chaves ACL, Gollob KJ, et al. *Trypanosoma cruzi* infection induces differential modulation of costimulatory molecules and cytokines by monocytes and T cells from patients with indeterminate and cardiac Chagas' disease. *Infect Immun*. American Society for Microbiology; 2007; 75: 1886–94. <https://doi.org/10.1128/IAI.01931-06> PMID: 17283096
37. Gomes JAS, Campi-Azevedo AC, Teixeira-Carvalho A, Silveira-Lemos D, Vitelli-Avelar D, Sathler-Avelar R, et al. Impaired phagocytic capacity driven by downregulation of major phagocytosis-related cell surface molecules elicits an overall modulatory cytokine profile in neutrophils and monocytes from the indeterminate clinical form of Chagas disease. *Immunobiology*. 2012; 217: 1005–16. <https://doi.org/10.1016/j.imbio.2012.01.014> PMID: 22387073
38. Sathler-Avelar R, Vitelli-Avelar DM, Elói-Santos SM, Gontijo ED, Teixeira-Carvalho A, Martins-Filho OA. Blood leukocytes from benznidazole-treated indeterminate chagas disease patients display an overall type-1-modulated cytokine profile upon short-term in vitro stimulation with *Trypanosoma cruzi* antigens. *BMC Infect Dis*. 2012; 12: 123. <https://doi.org/10.1186/1471-2334-12-123> PMID: 22625224

39. Alvarez MG, Postan M, Weatherly DB, Albareda MC, Sidney J, Sette A, et al. HLA Class I-T cell epitopes from trans-sialidase proteins reveal functionally distinct subsets of CD8+ T cells in chronic Chagas disease. *PLoS Negl Trop Dis*. 2008; 2: e288. <https://doi.org/10.1371/journal.pntd.0000288> PMID: [18846233](https://pubmed.ncbi.nlm.nih.gov/18846233/)
40. Souza PEA, Rocha MOC, Rocha-Vieira E, Menezes CAS, Chaves ACL, Gollob KJ, et al. Monocytes from patients with indeterminate and cardiac forms of Chagas' disease display distinct phenotypic and functional characteristics associated with morbidity. *Infect Immun*. 2004; 72: 5283–91. <https://doi.org/10.1128/IAI.72.9.5283-5291.2004> PMID: [15322024](https://pubmed.ncbi.nlm.nih.gov/15322024/)
41. Pinto BF, Medeiros NI, Teixeira-Carvalho A, Eloi-Santos SM, Fontes-Cal TCM, Rocha DA, et al. CD86 Expression by Monocytes Influences an Immunomodulatory Profile in Asymptomatic Patients with Chronic Chagas Disease. *Front Immunol*. 2018; 9: 454. <https://doi.org/10.3389/fimmu.2018.00454> PMID: [29599775](https://pubmed.ncbi.nlm.nih.gov/29599775/)
42. Stout RD, Jiang C, Matta B, Tietzel I, Watkins SK, Suttles J. Macrophages sequentially change their functional phenotype in response to changes in microenvironmental influences. *J Immunol*. 2005; 175: 342–9. PMID: [15972667](https://pubmed.ncbi.nlm.nih.gov/15972667/)
43. Mylonas KJ, Nair MG, Prieto-Lafuente L, Paape D, Allen JE. Alternatively activated macrophages elicited by helminth infection can be reprogrammed to enable microbial killing. *J Immunol*. 2009; 182: 3084–94. <https://doi.org/10.4049/jimmunol.0803463> PMID: [19234205](https://pubmed.ncbi.nlm.nih.gov/19234205/)
44. Sathler-Avelar R, Vitelli-Avelar DM, Massara RL, de Lana M, Pinto Dias JC, Teixeira-Carvalho A, et al. Etiological treatment during early chronic indeterminate Chagas disease incites an activated status on innate and adaptive immunity associated with a type 1-modulated cytokine pattern. *Microbes Infect*. 2008; 10: 103–13. <https://doi.org/10.1016/j.micinf.2007.10.009> PMID: [18248755](https://pubmed.ncbi.nlm.nih.gov/18248755/)
45. Campi-Azevedo AC, Gomes JAS, Teixeira-Carvalho A, Silveira-Lemos D, Vitelli-Avelar DM, Sathler-Avelar R, et al. Etiological treatment of Chagas disease patients with benznidazole lead to a sustained pro-inflammatory profile counterbalanced by modulatory events. *Immunobiology*. Elsevier GmbH.; 2015; 220: 564–74. <https://doi.org/10.1016/j.imbio.2014.12.006> PMID: [25648688](https://pubmed.ncbi.nlm.nih.gov/25648688/)